PHYSICAL REVIEW D **94,** 054004 (2016)

Ultraforward particle production from color glass condensate and Lund fragmentation

Javier L. Albacete,[1,*] Pablo Guerrero Rodríguez,[1,†] and Yasushi Nara[2,‡]

[1]*CAFPE and Departamento de Física Teórica y del Cosmos, Universidad de Granada, E-18071 Campus de Fuentenueva, Granada, Spain*

[2]*Akita International University, Yuwa, Akita-city 010-1292, Japan*

(Received 5 July 2016; published 6 September 2016)

We present an analysis of data on single inclusive pion production measured by the LHCf Collaboration in high-energy proton-proton and proton-nucleus at ultraforward rapidities, $8.8 \leq y \leq 10.8$. We also analyze forward RHIC data for calibration purposes. Our analysis relies on the use of a Monte Carlo event generator that combines a perturbative description of the elementary scattering process at partonic level based on the hybrid formalism of the color glass condensate with an implementation of hadronization in the framework of the Lund string fragmentation model. This procedure allows us to reach values of the momenta of the produced particles as low as detected experimentally, $p_t \sim 0.1$ GeV. We achieve a good description of single inclusive spectra of charged particles and neutral pions at the RHIC and the LHC, respectively, and nuclear modification factors for proton-lead collisions at the LHC. Our results add evidence to the idea that particle production in the domain of a very small Bjorken x is dominated by the saturation effects encoded in the unintegrated gluon distribution of the target. With forward particle production being of key importance in the development of air showers, we stress that this approach allows for a theoretically controlled extrapolation of our results to the scale of ultra-high-energy cosmic rays, thus serving as the starting point for future works on this topic.

DOI: 10.1103/PhysRevD.94.054004

I. INTRODUCTION

The detection and analysis of particle production in collision processes in the very forward region allows us to study wave functions of the colliding objects in extreme limits of the phase space. At partonic level, these collisions can be interpreted as mediated by a highly energetic valence quark from the projectile scattering off a soft or wee parton (typically a gluon) of the target hadron. After hadronization, the produced particles fly very close to the beam pipe until reaching the forward detectors. The Bjorken-x values probed in the scattering process can be estimated to be $x_{p,t} \approx (p_t/\sqrt{s})e^{\pm y}$ (more details follow below), where $\sqrt{s}$, p_t, and y refer to the collision energy, the transverse momentum, and the rapidity of the produced particle. In the kinematic range covered by LHCf, one has $\sqrt{s} = 7$ TeV, $p_t \lesssim 1$ GeV, and $8.8 \leq y \leq 10.8$, yielding the following Bjorken-x values for projectile and target: $x_p \sim 10^{-1} \sim 1$ and $x_t \sim 10^{-8} \sim 10^{-9}$. The latter values of Bjorken x are the smallest ever accessed in collider experiments. In this work we analyze forward production data in proton-proton and proton-nucleus collisions at the RHIC and the LHCf in terms of saturation physics and nonlinear small-x QCD evolution equations. In terms of evolution rapidity $Y = \ln(x_0/x)$, the simultaneous description of the RHIC (where the typical Bjorken-x values of the target are $\approx 10^{-3}$) and LHCf data implies testing such equations over a rapidity interval $\Delta Y \sim 14$.

From the theoretical point of view, it is well established that, at small values of Bjorken x, QCD enters a new regime governed by high gluon densities and the coherent dynamics of the soft color fields, consistently accounted for by the nonlinear renormalization group equations of QCD, the Balitsky-Kovchegov (BK) equation, and the Balitsky, Jalilian-Marian, Iancu, McLerran, Weigert, Leonidov, and Kovner (B-JIMWLK) equation [1–8]. The presence of nonlinear terms in the small-x evolution equations limits the growth rate of gluon number densities for modes of transverse momentum smaller than the saturation scale $Q_s(x)$. This novel, semihard dynamical scale marks the onset of nonlinear corrections in QCD evolution and leads to distinctive dynamical effects that, as we argue below, reflect in the ultraforward particle spectra measured by the LHCf Collaboration. In addition to theoretical arguments, there is by now an abundant corpus of phenomenological works that provides compelling evidence for the presence of saturation effects in currently available experimental data in a variety of collision systems: electron-proton, proton-proton, and heavy ion collisions. For a review, see, e.g., [9].

The LHC and RHIC forward particle production data have been analyzed in a series of previous works [10–12] in the framework of the color glass condensate (CGC) effective theory for high-energy QCD scattering

*albacete@ugr.es
†pgr@ugr.es
‡nara@aiu.ac.jp

(see, e.g., [13,14] for a review). Just as in this work, the above mentioned works relied on the use of hybrid factorization, well suited for the description of forward production processes or, equivalently, *dilute-dense* scattering, named thus for the strong asymmetry in the Bjorken-x values probed in the projectile and target. The main novelty of this work with respect to previous ones is the treatment of the hadronization process, which we describe in the framework of Lund string fragmentation. This procedure allows us to reach values of the momenta of the produced particles as low as detected experimentally, $p_t \sim 0.1$ GeV, and, therefore, opens the possibility of describing particle multiplicities. In turn, the description of the hadronization process in terms of the fragmentation functions used in previous works limits their applicability, by construction, to perturbatively large values of transverse momentum of the produced particle, $p_t \gtrsim 1$ GeV. Furthermore, we also take into account the possibility of multiple, simultaneous scatterings of different valence quarks with the dense glue of the target. The three main ingredients of our setup—namely, perturbative partonic production as given by the hybrid formalism, Lund fragmentation, and multiple scatterings—are embedded in a Monte Carlo event generator. The Monte Carlo code used here was first developed by one of the authors for the description of ultraforward pion production in proton-proton collisions at the LHC [15]. We shall extend it here to the case of proton-nucleus collisions and the study of the measured nuclear modification factors.

It should be noted that Monte Carlo event generators such as EPOS, PYTHIA, and SIBYLL provide a good description of ultraforward pion production in p-p and p-Pb collisions (see [16] and the references therein for details). While a detailed comparison between these different approaches and ours is beyond the scope of this paper, a main difference deserves to be mentioned: in our work the energy dependence of the single inclusive cross sections is described in terms of the nonlinear perturbative QCD evolution equations—a well-defined and controlled theoretical tool—whereas, in these other models, the energy dependence is encoded in free parameters adjusted in order to reproduce experimental data. Thus, although Monte Carlo event generators offer a more detailed quantitative description of large sets of data than what we shall present here, our approach provides new insight concerning the underlying dynamics of semihard processes, and it also manages to reduce the degree of modeling involved in the description of data. In this view, our approach is complementary to standard Monte Carlo event generators.

II. SETUP

A highly asymmetric collision in terms of the probed x values is also strongly asymmetric in the density of the colliding objects. In our case of study, the dilute system is given by the ensemble of valence partons in the proton projectile, which scatters off the highly dense, coherent glue in the target, be it a proton or a nucleus. In the hybrid formalism the large-x degrees of freedom of the proton are described in terms of usual parton distribution functions (PDFs) of collinear factorization which satisfy the momentum sum rule exactly and which exhibit a scale dependence given by the Dokshitzer-Gribov-Lipatov-Altarelli-Parisi (DGLAP) evolution equations. On the other hand, the small-x glue of the nucleus is described in terms of its unintegrated gluon distribution (UGD). The hybrid formalism was first proposed in [17] and, at partonic level, the cross section for quark or gluon production in the scattering off a dense gluonic target reads

$$\frac{d\sigma^{h_1 h_2 \to (q/g)X}}{dy d^2k} = \frac{K}{(2\pi)^2}\frac{\sigma_0}{2} x_1 f_{(q/g)/h_1}, (x_1,\mu^2) N_{(F/A),h_2}(x_2,k_t), \tag{1}$$

where $f_{(q/g),h_1}(x_1,\mu^2)$ is the PDF of quarks or gluons in the projectile h_1 evaluated at the scale μ, while $N_{(F/A),h_2}(x_2,k_t)$ refers to the UGD of the target in either the fundamental (F, for quarks) or adjoint (A, for gluons) representation. Eq. (1) is known as the Dumitru-Hayashigaki-Jalilian-Marian (DHJ) formula. The UGDs are related to the dipole scattering amplitude in coordinate space via a Fourier transform:

$$N_{(F/A)}(x,k_t) = \int d^2\mathbf{r} e^{-i\mathbf{k_t}\cdot\mathbf{r}}[1-\mathcal{N}_{(F/A)}(x,r)]. \tag{2}$$

We shall take the parametrization of the dipole scattering amplitude $\mathcal{N}(x,r)$ from the Albacete-Armesto-Milhano-Quiroga-Salgado (AAMQS) fits to data on the structure functions measured in e − p scattering at HERA [18,19]. The main dynamical input in those fits is the running coupling BK (RCBK) equation for the description of the x dependence of the dipole amplitudes [20–22]. The fit parameters are mostly related to the initial conditions for the evolution, set at the initial Bjorken-x value $x_0 = 10^{-2}$. In the AAMQS fits, they were chosen in the following form:

$$\mathcal{N}_F(x_0,r) = 1 - \exp\left[-\frac{(r^2Q_{s0}^2)^\gamma}{4}\log\left(\frac{1}{\Lambda r}+e\right)\right]. \tag{3}$$

The AAMQS fits provide a well constrained parametrization of the proton UGD. Similar to what has been done in previous works [23], we build the UGD of a nuclear target (lead or gold in our case), by simply rescaling the value of the initial saturation scale in Eq. (3) as: $Q_{s0,\text{nucleus}}^2 = A^{1/3}Q_{s0,\text{proton}}^2$, where A is the mass number of the target nucleus. The corresponding dipole scattering amplitudes in the adjoint representation are given, in the large-N_c limit, by $\mathcal{N}_A = 2\mathcal{N}_F - \mathcal{N}_F^2$. In this work we shall use the AAMQS sets corresponding to $\gamma = 1.101$, $Q_{s0}^2 = 0.157$ GeV^2 and $\gamma = 1.119$, $Q_{s0}^2 = 0.168$ GeV^2.

It turns out that the results for LHCf kinematics are not very sensitive to this particular choice and that other AAMQS sets yield a very similar description of the data.

As for the proton PDFs, we shall take the CTEQ5 leading order set [24] with a default factorization scale $\mu = \max\{k_t, Q_s\}$, where k_t is the transverse momentum acquired by the incoming parton as it multiply scatters the soft glue of the target. This choice ensures that primary partonic production can be described by means of perturbative tools. We cannot exclude that part of primary particle production could be of genuinely nonperturbative origin—especially for very small transverse momenta of the produced pions—and hence not amenable to description in terms of Eq. (1). However, the overall good description of the energy, rapidity, and partially transverse momentum of data (especially for the nuclear modification factor) reported below are indicative that those dynamical features of the process studied here are well accounted for by our approach. When applied to LHCf kinematics, our ansatz for the factorization scale ensures that it will always fall into the perturbative domain $\mu \gtrsim 1$ GeV since the saturation scale at the LHC ultraforward region is perturbatively large: $Q_s(x \sim 10^{-8}) \gtrsim 1$ GeV, both for proton and lead targets. Such is not the case in RHIC kinematics, where the saturation scale is considerably smaller and closer to its initial values $Q_{s0}^2 \sim 0.2$ GeV. In the latter case, we impose a momentum cutoff on the exchanged transverse momentum $k_{t,\min} = 1$ GeV. However, this cutoff is not necessary at the LHCf or, in other words, our results are insensitive to its precise value, as the scattering is dominated by higher transverse momenta, of the order of the saturation scale of the target $k_t \sim Q_s(x) \gtrsim 1$ GeV.

Finally, the factor σ_0 in Eq. (1) results from the integration over the impact parameter implicit in Eq. (2). In the mean field approach to treatment of the target geometry—proton or nucleus—that we shall adopt here, it carries the meaning of the average transverse size of the proton. Its value can be taken from the AAMQS fits where it was one of the free fit parameters ($\sigma_0/2 = 16.5$ mb). The K factor in Eq. (1) is not the result of any calculation. It has been added by hand to account for higher order corrections, possible nonperturbative effects, etc. In practice, we use it to adjust the normalization of theoretical curves to experimental data in phenomenological works. In an ideal situation, it should be equal to unity.

Before exploring more details on our implementation, a comment is in order: the degree of accuracy of the hybrid factorization formula as well as that of the nonlinear evolution equations describing the Bjorken-x dependence of the UGD of the target—running coupling BK in our case—has been considerably improved in recent times. For example, next-to-leading order (NLO) corrections to the cross-section equation (1) were calculated in [25,26]. Also, both the BK and B-JIMWLK evolution equations are now known at full NLO accuracy [27,28]. However, it was quickly noticed that the perturbative expansion of hadronic observables and evolution equations at NLO becomes unstable in certain regions of phase space [10,12,29], even leading to negative cross sections. Such unphysical behavior has been identified as arising from the increasing importance of double transverse momentum logarithms. Later works showed that the resummation of those collinear logs stabilizes the behavior of the perturbative series [30,31], even allowing a good phenomenological description of $e - p$ cross sections measured in HERA [32,33]. Recently, it was suggested that the kinematic corrections embodied in the resummation of large collinear logs can be accounted for through an appropriate subtraction of the rapidity divergence in the BK evolution for the target [34].

However, with the notable progress having been briefly reported above, we shall consider the hybrid formalism *only* at leading logarithmic accuracy together with LO DGLAP evolution and running coupling BK evolution to describe the scale dependence of the projectile PDF and the target UGD, respectively. Although a full NLO analysis of forward production data would be desirable—as all theoretical tools are now available—its phenomenological implementation should start by performing a global fit to e + p data at full NLO accuracy in order to obtain the UGD of a proton, which has not been carried out to date. Also, as shown in [10,12], NLO effects become increasingly important in the region of high transverse momentum and small to moderate evolution rapidities $Y = \ln(x_0/x)$. In this work we are interested in the opposite kinematic regime of very high evolution rapidities, $Y \sim 15$, and small transverse momentum scales, $k_t \lesssim Q_s(x)$. We expect then that the LO implementation of the hybrid factorization captures the main dynamical features of the collision process in the LHCf kinematic regime. This setup could be systematically improved using available theoretical progress, but we leave such a task for future work.

The three main ingredients of our setup—namely, primary, perturbative partonic production as given by Eq. (1), Lund fragmentation, and multiple scatterings—are embedded in a Monte Carlo event generator. At the partonic level, our Monte Carlo code generates quarks and gluons from $qg \to q$ and $gg \to g$ hard scatterings according to Eq. (1), along with initial and final state radiation based on DGLAP evolution. Multiple parton scattering is implemented in the eikonal model formalism [35–37], where we assume the probability distribution governing the number of independent hard scatterings to be a Poisson of mean n, with

$$n(b, s) = T_{\rm pp}(b)\sigma_{DHJ}(s). \tag{4}$$

n is the average number of partonic collisions per event. It depends on the invariant mass of the collision s through the integrated cross section σ_{DHJ}, and on the impact parameter

of the collision b through $T_{\rm pp}$, which is the spatial overlap of the colliding protons obtained as the convolution of two Gaussian functions:

$$T_{\rm pp}(b) = \frac{1}{4\pi B}\exp\left(-\frac{b^2}{4B}\right). \quad (5)$$

For every event, the impact parameter b is randomly generated in a range between 0 fm and

$$b_{\rm max} = \sqrt{\frac{\sigma_{nd}}{\pi}}, \quad (6)$$

which is the radius of a circle of area defined by the cross section of nondiffractive events, σ_{nd}. For collisions on nuclear targets, we substitute the target profile by a Gaussian with radius $R_{\rm A}^2 = R_{\rm p}^2 A^{2/3}$. Its convolution with the Gaussian profile of a proton yields

$$T_{\rm pA}(b) = \frac{A^{2/3}}{\pi R_{\rm p}^2 (A^{2/3}+1)}\exp\left(\frac{-b^2}{R_{\rm p}^2(A^{2/3}+1)}\right), \quad (7)$$

which is normalized to $A^{2/3}$. Other options for a nuclear spatial profile like the Woods-Saxon model were not considered in this work. The increase of the maximum impact parameter $b_{\rm max}$ allowed for nuclear targets is accounted for by the substitution of σ_{nd} into Eq. (6) by the cross-section values for the d-Au and p-Pb collisions given in [38,39].

Finally, the hadronization of the scattered partons into the finally observed hadrons is described in terms of the Lund string fragmentation model as embedded in the PYTHIA event generator. More specifically, PYTHIA6 [40] is used to arrange partons resulting from hard scattering and initial and final state radiation processes into strings; PYTHIA8.186 [41] is used to simulate their fragmentation into hadrons in the framework of the popcorn model. This particular choice of hadronization model turns out to be crucial for a good description of the data. Other possible choices, like the diquark model, result in much softer spectra of the produced pions, yielding worse agreement with the data. The remnants of the colliding hadrons are also arranged into strings (stretched between quark-diquark pairs). The fraction of the total energy x carried by the quark is chosen according to the probability density:

$$P(x) \propto \frac{(1-x)^{\alpha}}{\sqrt{4x^2 + c_{\rm min}^2}}, \quad (8)$$

where $c_{\rm min} = 2\langle m_q\rangle/\sqrt{s} = 0.6/\sqrt{s}$. For the α parameter we use the PYTHIA6 default value $\alpha = 3$. No primordial k_t distribution is considered, as in [15] it was shown to be unnecessary in this framework.

III. INCLUSIVE HADRON TRANSVERSE MOMENTUM SPECTRA AT THE RHIC

In this section we compare our results to experimental data in the kinematic range observed by two different RHIC detectors, namely, BRAHMS [42] and STAR [43]. The kinematic conditions achieved in the d-Au collisions performed at $\sqrt{s} = 200$ GeV at the RHIC are appropriate for a description in terms of the DHJ formula, provided that we focus on the high-rapidity region of the spectra, as depicted in Fig. 1. These fits act as a reference for calibration, as the data sets used have been largely studied in previous works based on the DHJ formula [11,15,44]. We build the PDF of the deuteron from the proton PDFs, assuming strict isospin symmetry. For each independent hard scattering, we calculate the multiplicity density of produced particles from Eq. (1) for the cross-section scaling by the nondiffractive cross section:

$$\frac{dN^{h_1h_2\to(q/g)X}}{dyd^2k} = \frac{1}{\sigma_{nd}}\frac{d\sigma^{h_1h_2\to(q/g)X}}{dyd^2k}. \quad (9)$$

We assume that the energy dependence of the nondiffractive cross section in Eq. (9) cancels out the energy dependence of the σ_0 factor in Eq. (1), even if these two objects are not necessarily the same. Any possible deviation from this assumption is lumped with the corresponding K factors.

We reach a rather good description of d-Au data on the spectra of negatively charged hadrons measured at pseudorapidities $\eta = 2.2$ and 3.2 by BRAHMS in minimum

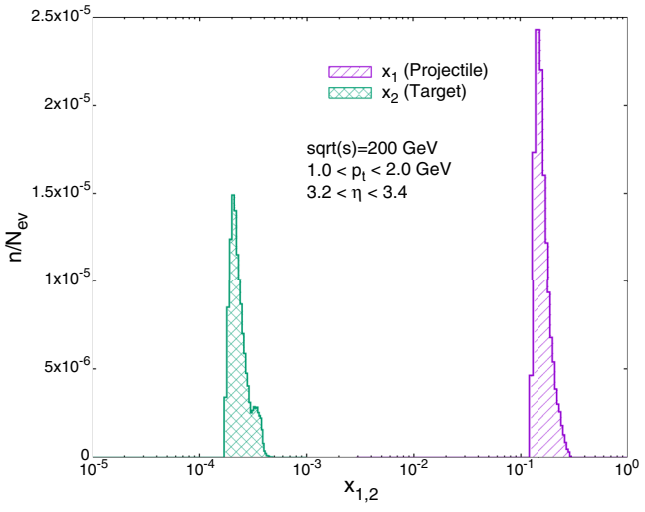

FIG. 1. Average distribution of Bjorken-x values for projectile and target and pseudorapidity of the produced particle $3.2 \le y \le 3.4$.

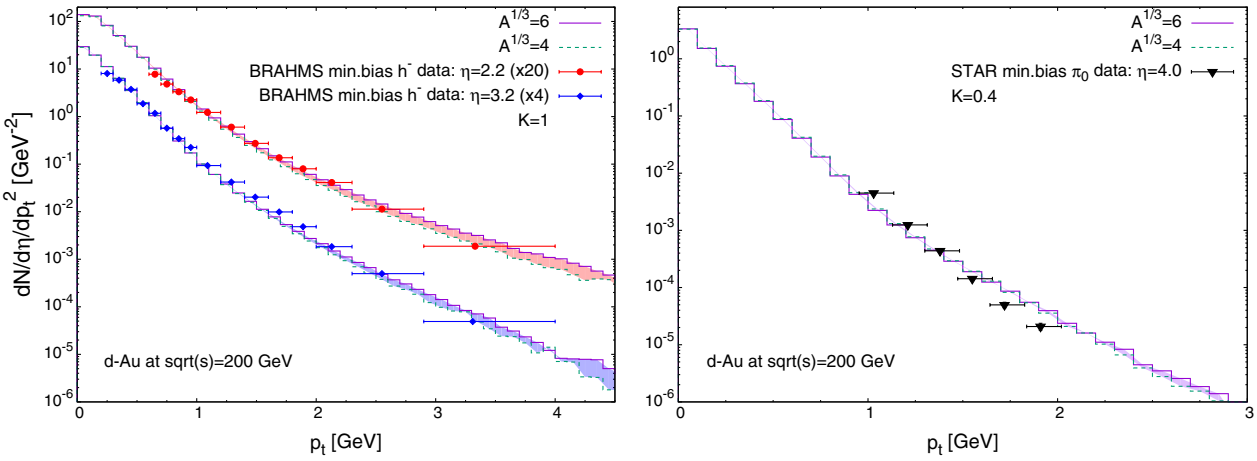

FIG. 2. (Left panel) Negatively charged hadron transverse momentum spectra at $\eta = 2.2$ and 3.2 in d-Au collisions at $\sqrt{s} = 200$ GeV measured by the BRAHMS Collaboration. (Right panel) Neutral pion spectra at $\eta = 4$ in d-Au collisions at $\sqrt{s} = 200$ GeV measured by the STAR Collaboration. Scale dependence between $Q_{s0}^2 = 0.157A^{1/3}$ GeV^2 with $A^{1/3} = 6$ and 4 is shown by the shaded areas.

bias collisions and also of STAR data on neutral pion production at $\eta = 4$; see Fig. 2. Our results are not very sensitive to the specific value of the number of participant nucleons in the collision, which, in the mean field treatment of nuclear geometry performed here, is given by $N_{\rm part} \approx A^{1/3}$. The most remarkable, and completely new, feature of our result is that, by means of the Lund fragmentation mechanism implemented in our Monte Carlo, we can reach values of the transverse momentum of the produced particle as low as detected experimentally, $p_{t,\rm min} \sim 0.2$ GeV. Previous approaches relied on the use of fragmentation functions to describe the hadronization process. Hence, by construction, they could only access the regime of perturbatively high transverse momenta, $p_{t,\rm min} \gtrsim 1$ GeV, where these functions are defined. BRAHMS data is well described with a K factor of $K = 1$. However, STAR data on neutral pions can only be described with a K factor of $K = 0.4$, exactly the same value obtained in a previous analysis of the data.

IV. INCLUSIVE HADRON TRANSVERSE MOMENTUM SPECTRA AT LHCf

In this section we compare our results with the preliminary data on neutral pion production measured by the LHCf Collaboration in p-p and p-Pb collisions at $\sqrt{s} = 7$ and 5.02 TeV, respectively [16]. The ultrahigh rapidity range available in this experiment ($8.8 \leq y \leq 10.8$) is appropriate for a description in terms of the DHJ formula, as shown in Fig. 3, where we plot the distribution of Bjorken-x values contributing to these collisions from the projectile and the target, respectively. They are peaked in $x_p \approx 0.1$ and $x_t \approx 10^{-8}$, which indicates a much stronger dilute-dense asymmetry than in the RHIC case (Fig. 1).

Similarly to the previous analysis presented in [15], we obtain a good description of p-p data for all rapidities; see Fig. 4. Importantly, the K factor used for a description of the data is exactly the same as the one used for the description of the BRAHMS data, $K = 1$. This is an important result, as it indicates that the energy evolution from the RHIC to the LHC, equivalent to more than ten units in evolution rapidity, $\Delta Y \gtrsim 14$, is well accounted for by the theoretical tools in our approach—namely, the running coupling BK evolution for the x dependence of the UGDs. For the sake of illustration, in Fig. 4 we also show the partonic spectra generated prior to the hadronization process, where it can be seen that the partonic and hadronic spectra have a very similar shape at all rapidities. This observation lends support to the idea of a parton-hadron duality. Equivalently, it shows that the energy, rapidity, and transverse momentum dependence of the single inclusive spectra in our model is mostly shaped

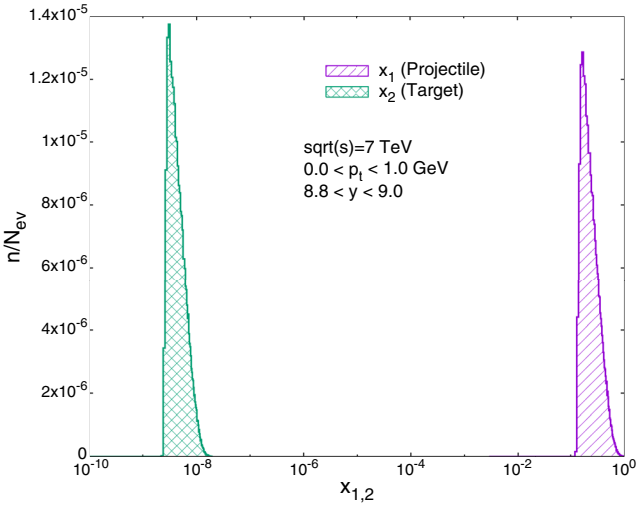

FIG. 3. Average distribution of Bjorken-x values for projectile and target and rapidity of the produced particle $8.8 \leq y \leq 9.0$.

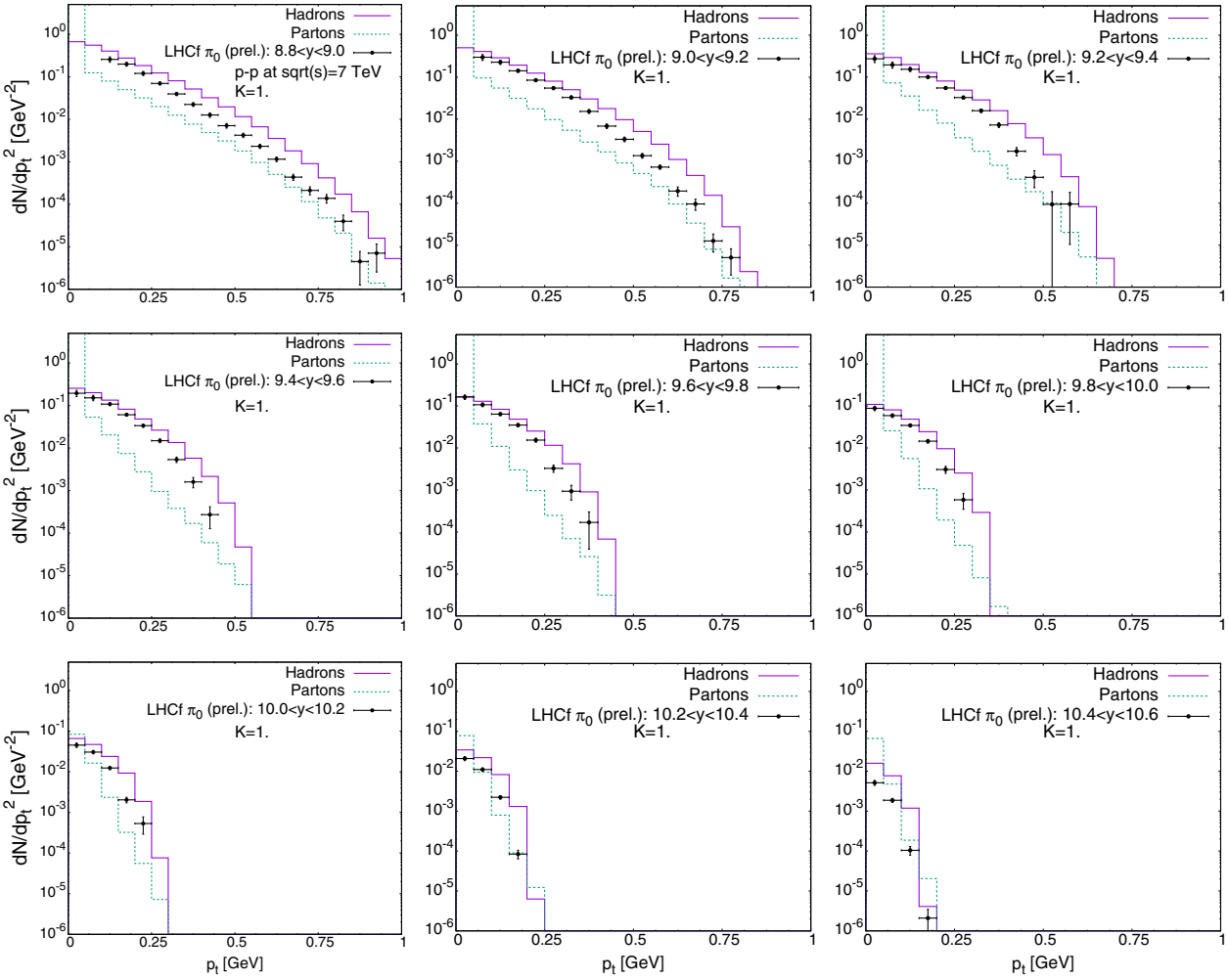

FIG. 4. Neutral pion transverse momentum spectra in the rapidity range $8.9 < y < 10.6$ in p-p collisions at $\sqrt{s} = 7$ TeV. Also shown are the corresponding partonic spectra (the dashed lines).

by the perturbative QCD ingredients in our calculation—namely, PDFs and RCBK-evolved UGDs. The main role of the fragmentation dynamics encoded in the Lund model is to smear the partonic p_t spectrum and an increase of the multiplicity due to the fragmentation process. As a comment, it should be noted that the bump observed for the lowest momentum bin is due to the contribution of projectile remnants not participating in the hard scattering. We also find good agreement of the neutral pion spectra measured in p-Pb collisions; see Fig. 5. In this case our theoretical result is a bit below the data at the highest values of transverse momenta. Again, we have used a K factor $K = 1$ for its description. As shown in Fig. 5, a slightly larger value of the K factor, $K = 1.5$, results in a slightly better description of the data.

It is apparent from Figs. 4 and 5 that the description of LHCf data, although good, is not as good as the one obtained for the RHIC data discussed in the previous section. Certainly, it is open for improvement. We find several reasons for this partial disagreement. First, a reduced K factor $K < 1$ at the LHCf would improve the description of the p-p data. As mentioned in Sec. II, higher order corrections to our CGC setup for particle production are now available. It is known that these higher order corrections tend to result in a reduced growth of UGDs with increasing collision energy, hence effectively reducing the K factor at small x. Second, LHCf kinematics lie very close to the kinematic limit $x_F \to 1$, especially at high transverse momentum. It has been argued that factorization theorems break down in the vicinity of $x_F \to 1$, resulting in induced, p_t-dependent energy loss and a distortion of the spectra. Finally, the details of the fragmentation process could also be tuned for a better description of the data. Also, the highest p_t values probe the projectile PDFs in $x_p \to 1$, where uncertainties are high. All of these effects could be systematically explored in order to fix a fully operational phenomenological framework. However, such tasks are beyond the scope of this paper and are left for future work.

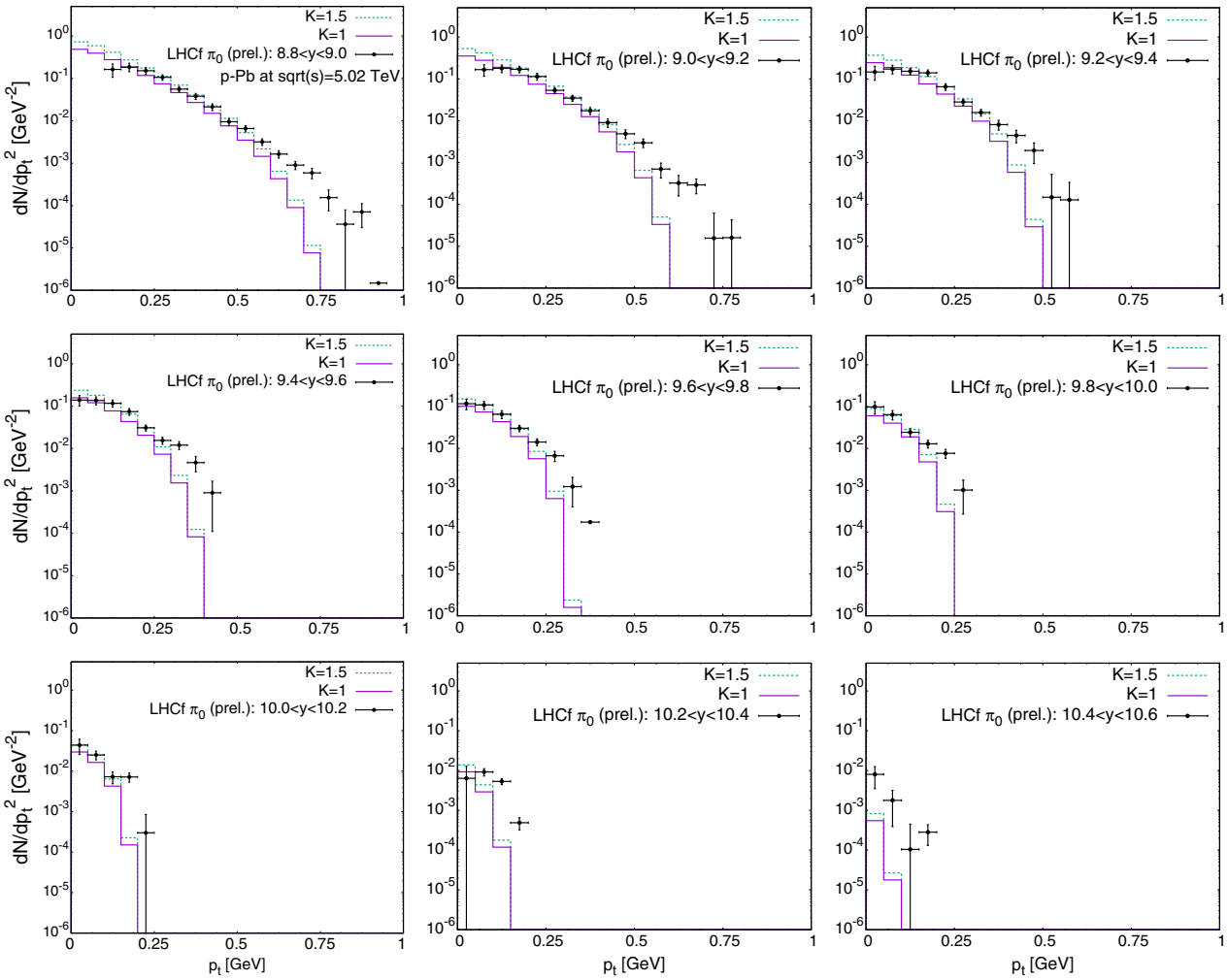

FIG. 5. Neutral pion transverse momentum spectra in the rapidity range $8.9 < y < 10.6$ in p-Pb collisions at $\sqrt{s_{NN}} = 5.02$ TeV measured at the LHCf detector. Solid and dashed lines correspond to the K factors $K = 1$ and $K = 1.5$, respectively.

V. NUCLEAR MODIFICATION FACTOR AT LHCf

Finally, in this section we present our results for the nuclear modification factor $R_{\text{p-Pb}}$, defined as follows:

$$R^{\pi^0}_{\text{p-Pb}} \equiv \frac{\sigma^{\text{pp}}_{\text{inel}}}{\langle N_{\text{coll}}\rangle \sigma^{\text{pPb}}_{\text{inel}}} \frac{Ed^3\sigma^{\text{pPb}}/d^3p}{Ed^3\sigma^{\text{pp}}/d^3p} = \frac{1}{\langle N_{\text{coll}}\rangle} \frac{dN^{\text{pPb}\to\pi^0 X}/dyd^2p_t}{dN^{\text{pp}\to\pi^0 X}/dyd^2p_t}, \tag{10}$$

where $Ed^3\sigma^{\text{pPb}}/dp^3$, $Ed^3\sigma^{\text{pp}}/dp^3$ are the inclusive cross sections of neutral pion production in p-Pb and p-p collisions, respectively, and $\langle N_{\text{coll}}\rangle$ is the average number of nucleon-nucleon scatterings in a p-Pb collision. We shall use the same value of $\langle N_{\text{coll}}\rangle$ as was used in the experimental analysis [16], obtained from a Monte Carlo Glauber simulation: $\langle N_{\text{coll}}\rangle = 6.9$. Also, it should be kept in mind that the experimental data set for $\sqrt{s} = 5.02$ TeV is obtained after interpolating p-p data from 2.76 and 7 TeV collision energies.

One remarkable feature of experimental data is the approximate flatness of the $R^{\pi^0}_{\text{p-Pb}}$ over the entire measured rapidity range. Actually, a constant value $R^{\pi^0}_{\text{p-Pb}} = 1/\langle N_{\text{coll}}\rangle \approx 0.15$ is compatible with data for all y's (as shown in Fig. 6). This would immediately imply that the multiplicity density in p-p collisions is approximately equal to the one in p-Pb collisions [see the right-hand side of Eq. (10)]:

$$\frac{dN^{pp\to\pi^0 X}}{dyd^2p_t} \approx \frac{dN^{pPb\to\pi^0 X}}{dyd^2p_t}. \tag{11}$$

Certainly, a more refined analysis of the data would probably indicate a decreasing behavior of $R^{\pi^0}_{\text{p-Pb}}$ with an increasing rapidity of the detected pions. However, such a rate of change is much smaller than the one observed at RHIC energies in a similar range of transverse momenta. This purely empirical observation is well accounted for by

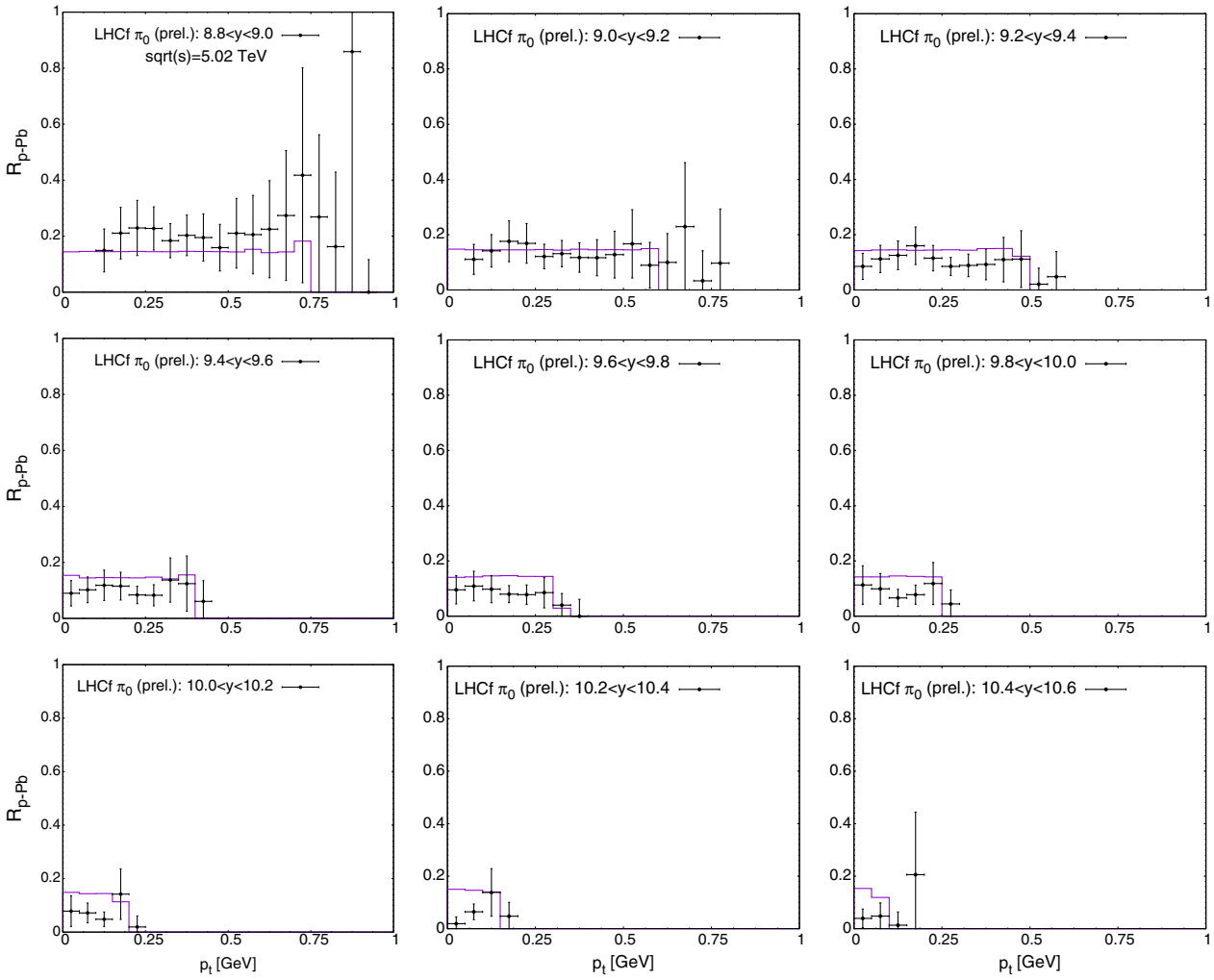

FIG. 6. Nuclear modification factor for neutral pion production at $\sqrt{s_{NN}} = 5.02$ TeV. The data points were taken from [16]. Since there is no neutral pion transverse momentum spectra measurement available for p-p collisions at $\sqrt{s} = 5.02$ TeV, it is derived by interpolation of data sets obtained from p-p collisions at $\sqrt{s} = 7$ and 2.76 TeV, which are included in that paper.

our calculations. In terms of saturation physics, this result can be immediately related to the asymptotic properties of the solution of the BK equation, which are used to describe the x dependence of the UGDs of the proton and lead targets. At partonic level, Eq. (11) can be written as

$$\langle n_{\text{p-Pb}} \rangle_b N^{\text{Pb}}_{(F/A)} \approx \langle n_{\text{p-p}} \rangle_b N^{\text{p}}_{(F/A)}, \tag{12}$$

where $N^{\text{Pb}}_{(F/A)}$, $N^{\text{p}}_{(F/A)}$ are the UGDs corresponding to proton and nucleus targets, and $\langle n_{\text{p-Pb}} \rangle_b$, $\langle n_{\text{p-p}} \rangle_b$ are the average number of independent hard collisions per p-p and p-Pb events integrated over impact parameter. Because of the normalization of the spatial overlap function for proton-nucleus collisions, T_{pA}, the integration of Eq. (4) over b yields

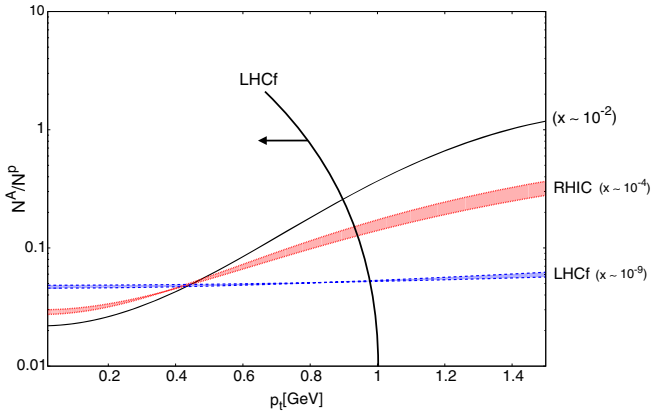

FIG. 7. Ratio of RCBK-evolved unintegrated gluon distributions for proton and lead targets for the different x ranges observed at the RHIC and the LHC.

$$\langle n_{\text{p-Pb}}\rangle_b = A^{2/3}\langle n_{\text{p-p}}\rangle_b. \quad (13)$$

Applying this expression to Eq. (12) and also neglecting the difference in the factorization scales for p or Pb scattering, we get

$$\frac{N^{\text{Pb}}_{(F/A)}}{N^{\text{p}}_{(F/A)}} = \frac{1}{A^{2/3}}. \quad (14)$$

This behavior is well realized by the RCBK-evolved UGDs used in this work. As shown in Fig. 7, the ratio of lead over proton UGDs takes a constant value $1/A^{2/3} \approx 0.03$ in the entire k_t range probed by the LHCf data studied here. We interpret the fact that the experimental data on the nuclear modification factor reproduces this constant behavior over the whole range of rapidity as an indication of the prevalence of saturation effects in the probed kinematic regime by the LHCf. In turn, the analogous ratio, when plotted for the kinematic regime relevant for forward RHIC data, exhibits a growing behavior with an increasing transverse momentum, in the very same fashion as the corresponding nuclear modification factor. We conclude that RHIC forward kinematics falls outside the universality regime of small-x evolution. Rather, RHIC kinematics test nonlinear evolution in the preasymptotic regime.

VI. DISCUSSION

In this work we have shown that it is possible to obtain a good description of particle production (single neutral pion spectrum) in the very forward region of the LHC and down to the lowest values of transverse momentum experimentally accessed by the LHCf Collaboration ($p_t \lesssim 0.1$ GeV). We do so via the combination of a perturbative description of the elementary partonic scattering process with a nonperturbative *stringy* characterization of the fragmentation and decay of the *hard* partons. Our results provide yet another indication for the presence of—and need for—saturation effects to correctly describe presently available experimental data dominated by the contribution of very small-x gluons. Indeed, the good and simultaneous description of p-p and p-Pb data and, in particular, of the nuclear modification $R^{\pi^0}_{p-Pb}$ factor affords a neat theoretical interpretation in terms of saturation physics. The flatness and approximately constant behavior of the observed R_{pPb} over the wide range of rapidities covered by the data can be related to the asymptotic properties of the solutions of the BK equation and, in particular, to the existence of universal solutions at sufficiently small x.

Aside from the description of the data discussed in this work, the fact that the main features of ultraforward production data—even for very small transverse momentum of the produced particles—can be understood in terms of perturbative tools may provide new insights in the field of ultra-high-energy cosmic rays (UHECRs). There, the main features of the air showers developed after the primary collisions in the upper atmosphere are determined to a large extent by the hadronic collision properties, particularly by the total cross section, the forward multiplicity, the charm production, the inelasticity, etc. [45]. Thus, the availability of theoretically controlled tools for extrapolating from the well constrained collision energy domain probed at the LHC to that of UHECRs is necessary to reduce the inherent uncertainty associated with the extrapolation itself and, thereby, also the uncertainty associated with the present analysis of the primary mass composition of UHECRs. We propose that the use of nonlinear renormalization group equations of QCD (like the BK equation employed in this work) may be an useful tool in the analysis of UHECRs, and we plan to extend our studies in this direction in future work.

ACKNOWLEDGMENTS

This work is funded by a FP7-PEOPLE-2013-CIG Grant of the European Commission, Grant No. QCDense/631558 and by Ramón y Cajal and MINECO Projects No. RYC-2011-09010 and No. FPA2013-47836.

[1] J. Jalilian-Marian, A. Kovner, A. Leonidov, and H. Weigert, The Wilson renormalization group for low x physics: Towards the high density regime, Phys. Rev. D **59**, 014014 (1998).

[2] J. Jalilian-Marian, A. Kovner, and H. Weigert, The Wilson renormalization group for low x physics: Gluon evolution at finite parton density, Phys. Rev. D **59**, 014015 (1998).

[3] A. Kovner, J. G. Milhano, and H. Weigert, Relating different approaches to nonlinear QCD evolution at finite gluon density, Phys. Rev. D **62**, 114005 (2000).

[4] H. Weigert, Unitarity at small Bjorken x, Nucl. Phys. **A703**, 823 (2002).

[5] E. Iancu, A. Leonidov, and L. D. McLerran, Nonlinear gluon evolution in the color glass condensate. I, Nucl. Phys. **A692**, 583 (2001).

[6] E. Ferreiro, E. Iancu, A. Leonidov, and L. McLerran, Nonlinear gluon evolution in the color glass condensate. II, Nucl. Phys. **A703**, 489 (2002).

[7] I. Balitsky, Operator expansion for high-energy scattering, Nucl. Phys. **B463**, 99 (1996).

[8] Y. V. Kovchegov, Small-x F_2 structure function of a nucleus including multiple Pomeron exchanges, Phys. Rev. D **60**, 034008 (1999).
[9] J. L. Albacete and C. Marquet, Gluon saturation and initial conditions for relativistic heavy ion collisions, Prog. Part. Nucl. Phys. **76**, 1 (2014).
[10] J. L. Albacete, A. Dumitru, H. Fujii, and Y. Nara, CGC predictions for p + Pb collisions at the LHC, Nucl. Phys. **A897**, 1 (2013).
[11] J. L. Albacete and C. Marquet, Single inclusive hadron production at RHIC and the LHC from the color glass condensate, Phys. Lett. B **687**, 174 (2010).
[12] A. M. Stasto, B.-W. Xiao, and D. Zaslavsky, Towards the Test of Saturation Physics beyond Leading Logarithm, Phys. Rev. Lett. **112**, 012302 (2014).
[13] H. Weigert, Evolution at small x: The color glass condensate, Prog. Part. Nucl. Phys. **55**, 461 (2005).
[14] F. Gelis, E. Iancu, J. Jalilian-Marian, and R. Venugopalan, The color glass condensate, Annu. Rev. Nucl. Part. Sci. **60**, 463 (2010).
[15] W.-T. Deng, H. Fujii, K. Itakura, and Y. Nara, Forward hadron productions in high energy pp collisions from a Monte-Carlo generator for color glass condensate, Phys. Rev. D **91**, 014006 (2015).
[16] O. Adriani *et al.*, Measurements of longitudinal and transverse momentum distributions for neutral pions in the forward-rapidity region with the LHCf detector, Phys. Rev. D **94**, 032007 (2016).
[17] A. Dumitru, A. Hayashigaki, and J. Jalilian-Marian, The color glass condensate and hadron production in the forward region, Nucl. Phys. **A765**, 464 (2006).
[18] J. L. Albacete, N. Armesto, J. G. Milhano, and C. A. Salgado, Nonlinear QCD meets data: A global analysis of lepton-proton scattering with running coupling Balitsky-Kovchegov evolution, Phys. Rev. D **80**, 034031 (2009).
[19] J. L. Albacete, N. Armesto, J. G. Milhano, P. Quiroga-Arias, and C. A. Salgado, AAMQS: A non-linear QCD analysis of new HERA data at small-x including heavy quarks, Eur. Phys. J. C **71**, 1705 (2011).
[20] Y. Kovchegov and H. Weigert, Triumvirate of running couplings in small-x evolution, Nucl. Phys. **A784**, 188 (2007).
[21] I. I. Balitsky, Quark contribution to the small-x evolution of color dipole, Phys. Rev. D **75**, 014001 (2007).
[22] J. L. Albacete and Y. V. Kovchegov, Solving high energy evolution equation including running coupling corrections, Phys. Rev. D **75**, 125021 (2007).
[23] J. L. Albacete and A. Dumitru, A model for gluon production in heavy-ion collisions at the LHC with rcBK unintegrated gluon densities, arXiv:1011.5161.
[24] J. Pumplin, D. R. Stump, J. Huston, H.-L. Lai, P. Nadolsky, and W.-K. Tung, New generation of parton distributions with uncertainties from global QCD analysis, J. High Energy Phys. 07 (2002) 012.
[25] T. Altinoluk, N. Armesto, G. Beuf, A. Kovner, and M. Lublinsky, Single-inclusive particle production in proton-nucleus collisions at next-to-leading order in the hybrid formalism, Phys. Rev. D **91**, 094016 (2015).
[26] G. A. Chirilli, B.-W. Xiao, and F. Yuan, Inclusive hadron productions in pA collisions, Phys. Rev. D **86**, 054005 (2012).
[27] I. Balitsky and G. A. Chirilli, Next-to-leading order evolution of color dipoles, Phys. Rev. D **77**, 014019 (2008).
[28] I. Balitsky and G. A. Chirilli, Rapidity evolution of Wilson lines at the next-to-leading order, Phys. Rev. D **88**, 111501 (2013).
[29] T. Lappi and H. Mäntysaari, Direct numerical solution of the coordinate space Balitsky-Kovchegov equation at next to leading order, Phys. Rev. D **91**, 074016 (2015).
[30] E. Iancu, J. Madrigal, A. Mueller, G. Soyez, and D. Triantafyllopoulos, Resumming double logarithms in the QCD evolution of color dipoles, Phys. Lett. B **744**, 293 (2015).
[31] T. Lappi and H. Mäntysaari, Next-to-leading order Balitsky-Kovchegov equation with resummation, Phys. Rev. D **93**, 094004 (2016).
[32] J. L. Albacete, Resummation of double collinear logs in BK evolution versus HERA data, arXiv:1507.07120.
[33] E. Iancu, J. D. Madrigal, A. H. Mueller, G. Soyez, and D. N. Triantafyllopoulos, Collinearly-improved BK evolution meets the HERA data, Phys. Lett. B **750**, 643 (2015).
[34] B. Ducloué, T. Lappi, and Y. Zhu, Single inclusive forward hadron production at next-to-leading order, Phys. Rev. D **93**, 114016 (2016).
[35] J. M. Butterworth, J. R. Forshaw, and M. H. Seymour, Multiparton interactions in photoproduction at HERA, Z. Phys. C **72**, 637 (1996).
[36] L. Durand and P. Hong, QCD and Rising Cross Sections, Phys. Rev. Lett. **58**, 303 (1987).
[37] L. Durand and H. Pi, Semihard QCD and high-energy pp and $\bar{p}p$ scattering, Phys. Rev. D **40**, 1436 (1989).
[38] B. Z. Kopeliovich, Transparent nuclei and deuteron gold collisions at RHIC, Phys. Rev. C **68**, 044906 (2003).
[39] V. Khachatryan *et al.* (CMS Collaboration), Measurement of the inelastic cross section in proton-lead collisions at $\sqrt{s_{\mathrm{NN}}} = 5.02$ TeV, Phys. Lett. B **759**, 641 (2016).
[40] T. Sjostrand, S. Mrenna, and P. Z. Skands, PYTHIA6.4 physics and manual, J. High Energy Phys. 05 (2006) 026.
[41] T. Sjostrand, S. Mrenna, and P. Z. Skands, A brief introduction to PYTHIA8.1, Comput. Phys. Commun. **178**, 852 (2008).
[42] I. Arsene *et al.* (BRAHMS Collaboration), Evolution of the Nuclear Modification Factors with Rapidity and Centrality in $d + Au$ Collisions at $\sqrt{N^S N} = 200$ GeV, Phys. Rev. Lett. **93**, 242303 (2004).
[43] J. Adams *et al.* (STAR Collaboration), Forward Neutral Pion Production in $p + p$ and $d + Au$ Collisions at $\sqrt{s_{NN}} = 200$ GeV, Phys. Rev. Lett. **97**, 152302 (2006).
[44] J. Jalilian-Marian and A. H. Rezaeian, Hadron production in pA collisions at the LHC from the color glass condensate, Phys. Rev. D **85**, 014017 (2012).
[45] R. Ulrich, R. Engel, S. Müller, T. Pierog, F. Schüssler, and M. Unger, Sensitivity of extensive air showers to features of hadronic interactions at ultra-high energies, arXiv:0906.0418.